Available online at www.sciencedirect.com
ScienceDirect
Journal of the European Ceramic Society 28 (2008) 123–131
www.elsevier.com/locate/jeurceramsoc

Effect of sintering conditions on the pyrochlore phase content in PMN–PFN ceramics prepared by sol–gel process

H. Bruncková *, Ľ. Medvecký, J. Mihalik

Institute of Materials Research, Slovak Academy of Sciences, Watsonova 47, 043 53 Košice, Slovak Republic

Available online 17 October 2007

Abstract

Lead magnesium niobate–lead iron niobate [$(1-x)Pb(Mg_{1/3}Nb_{2/3})O_3$–$xPb(Fe_{1/2}Nb_{1/2})O_3$, $(1-x)$PMN–xPFN] system, where $x = 0.0$–1.0, was prepared using sol–gel synthesis by mixing acetates Pb, Mg and Fe with Nb-ethylene glycol-tartarate complex at 80 °C. Single pyrochlore phase ($Pb_{1.83}Mg_{0.29}Nb_{1.71}O_{6.39}$ or $Pb_3Nb_4O_{13}$) was formed by the calcination of gels at 600 °C. Average particle sizes of pure PMN and PFN powders were ∼80 and 150 nm. The pyrochlore phases were partially decomposed to perovskite phase at sintering temperatures of 1150 and 1250 °C. The maximum bulk density in ceramic samples increased with both sintering temperature and the content of PFN phase in samples but despite these facts—the volume fractions of porosity were too high in all prepared samples. From the point of view of perovskite phase content, the optimum sintering temperature of PMN–PFN is shifted from 1200 to 1150 °C in comparison with the sample with PMN stoichiometry. Low values of ε_r were measured in low density samples with high pyrochlore content and this characteristic is probably the main factor affecting ε_r in prepared ceramics. In microstructures of PMN–PFN ceramics sintered at 1150 °C at different times, the bimodal grain size distribution was observed with small grains of globular shape and larger grains of regular or octahedral shape. The results of EDX and XRD analysis showed that the more complex types of pyrochlore phases were present in ceramics.

Keywords: Sol–gel; Sintering; Dielectric properties

1. Introduction

Lead based complex perovskites with the general formula $A(B'B'')O_3$ such as $Pb(Mg_{1/3}Nb_{2/3})O_3$ (PMN) and $Pb(Fe_{1/2}Nb_{1/2})O_3$ (PFN) have received considerable attention since the late 1970s and have been applied recently in multilayer ceramic capacitors (MLCCs) and electrostrictive actuators.[1–4] Lead magnesium niobates are the most promising and the best known lead based ferroelectric relaxor materials. One of the Soviet groups as the first developed these materials in the late 1950s.[5] Lead iron niobate is interesting as a component in commercial electroceramic materials.

It is very difficult to fabricate the pure perovskite ABO_3 (pv) PMN and PFN phases without the formation of the undesirable pyrochlore $A_2B_2O_6$ (py) phase, which degrades the dielectric properties of ceramics. To obtain single-phase PMN, four various synthesis techniques: basic process (conventional techniques),[6] double-step method (columbite[7] and wolframite[8]), wet chemical route,[9] and salt-based method.[10] In the conventional method (solid state reaction) the oxides (PbO, MgO and Nb_2O_5) are weighted and mixed under dry or wet conditions. The powder is calcined at 800 °C and after calcination pellets fired at 900 °C. The pyrochlore phase is formed during the synthesis of PMN powder by mixed oxide route. Lejeune and Boilot[6] have reported the formation of three types pyrochlore $Pb_3Nb_4O_{13}$, $Pb_2Nb_2O_7$ and $Pb_3Nb_2O_8$. Swartz and Shrout[7] in two-stage process in columbite route, MgO and Nb_2O_5 are reacted at 1000 °C to a columbite $MgNb_2O_6$ phase, which is then reacted with PbO at 800 °C to PMN powder with ∼5% pyrochlore phase. Swartz et al.[4] later prepared pyrochlore-free PMN powder by using excess MgO. Ananta and Thomas[11] developed two-stage mixed oxide synthetic routes for the preparation of single phases of lead-based complex perovskite PMN and PFN and two complex perovskite compounds at selected compositions in the PMN–PFN pseudo-binary system were prepared and characterized[12]. PMN is also synthetized by various wet chemical processing routes such as sol–gel,[9,13–16] combustion synthesis,[17,18] coprecipitation,[19] molten salt synthesis,[20] citrate gel,[21,22] partial oxalate, [23,24] polymerized complex,[24,25] citrate complex[26] and a niobium tartarate complex[27] meth-

* Corresponding author.
E-mail address: hbunckova@imr.saske.sk (H. Bruncková).

0955-2219/$ – see front matter © 2007 Elsevier Ltd. All rights reserved.
doi:10.1016/j.jeurceramsoc.2007.09.026

ods. The combination of the partial oxalate method with the columbite route and the Pechini method was used to obtain PMN powder at low temperature.[28] The Pechini method is based on the formation of metallic complexes (Nb complex) with carboxylic acid as ligand, normally citric or tartaric acid followed by a polymerization reaction with a polyalcohol (e.g. ethylene glycol) generating polyester.

Chaput et al.[9] prepared PMN phase by a sol–gel method using alkoxide precursors. The pyrochlore phase was completely transformed into PMN pv phase around 700 °C. A colloidal sol–gel route represents the preparation of PMN and PMN–PFN systems from metal chlorides and nitrates.[29] The powder precursors were calcined at 300 °C and sintered between 850 and 1100 °C. Besides the sol–gel synthesis, the calcination temperature and pyrolysis conditions influence the formation of the final perovskite phase. This affect densification behaviour, microstructure development and dielectric properties in ceramic perovskite systems. As the optimum sintering conditions (temperature and time) using a mixed oxide route have been recommended for PMN ceramics −1150 °C/1 h,[30] 1275 °C/2 h,[31,32] using a partial oxalate method −1200 °C/2 h,[33] for the preparation of PFN ceramics lower temperatures of 1175 °C/2 h[34] and temperatures of 1050–1200 °C/1 h in the case of PMN–PFN ceramics.[35] High sintering temperature (of up to 1275 and 1175 °C for PMN and PFN, respectively) or a long sintering times up to 6 h were adopted[35].

It known that a stable pyrochlore phases are often formed in PMN and PFN ceramics. The presence of py phases causes decrease in the dielectric permitivity. Two types of pyrochlore phases have been found to co-exist with the major perovskite phase in the PMN system, i.e. $Pb_{1.83}Mg_{0.29}Nb_{1.71}O_{6.39}$ and $Pb_3Nb_4O_{13}$. In PFN system, $PbFe_8O_{13}$, $Pb_2Fe_{1.2}Nb_{0.8}O_{5.5}$ and $Pb_3Fe_4Nb_4O_{21}$ pyrochlore phases were found.[32,34] The dielectric properties of a material depend on frequency, temperature at which are measured, pyrochlore phase content, sintering temperature and time. The maximum of dielectric permitivity is shifted to higher temperature with the content of PFN in PMN–PFN ceramics (pure PMN ceramics: $\varepsilon_r \sim 16{,}000$, $T_c = -10$ °C; pure PFN ceramics: $\varepsilon_r \sim 21{,}000$, $T_c = 110$ °C).[35] In producing PMN ceramics with high dielectric permitivity, the formation pyrochlore phase (with low $\varepsilon_r \sim 200$) is crucial factor.

The present paper describes the preparation of PMN–PFN ceramics using the sol–gel synthesis by mixing acetates Pb, Mg and Fe with Nb-ethylene glycol-tartarate complex. The influence of sintering temperature and time on the phase composition and microstructure in the final PMN–PFN ceramics has been investigated.

2. Experimental

$(1-x)$PMN–xPFN precursors, where $x = 0.0$–1.0, were prepared by the sol–gel synthesis according to diagram in Fig. 1. Lead acetate trihydrate $Pb(OAc)_2{\cdot}3H_2O$, magnesium hydroxycarbonate $4[MgCO_3]{\cdot}Mg(OH)_2{\cdot}5H_2O$ and iron nitrate $Fe(NO)_3{\cdot}9H_2O$ were mixed in solvent acetic acid (AcOH) at

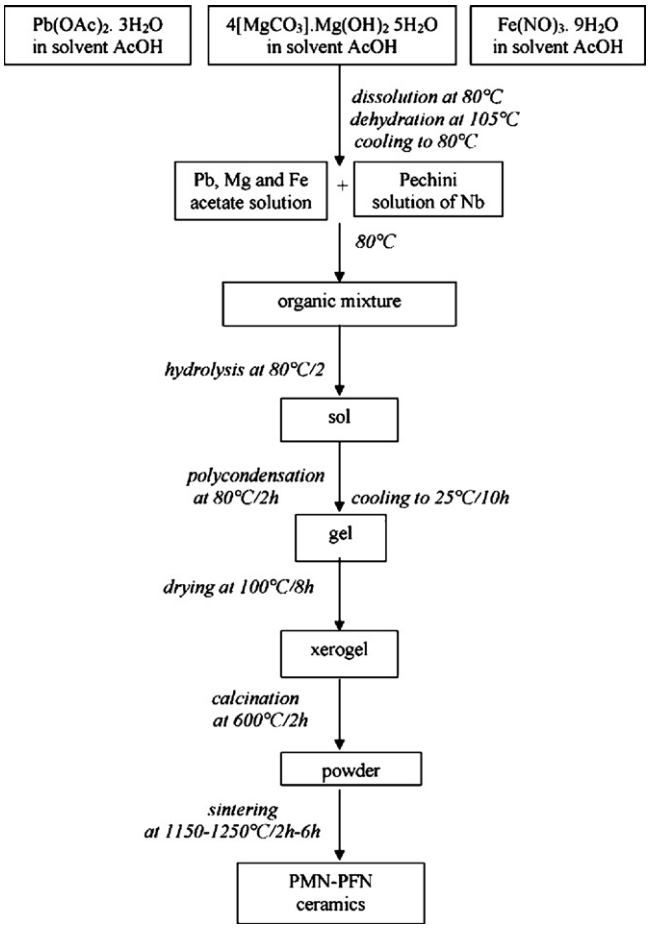

Fig. 1. A scheme for preparation of PMN–PFN ceramics by sol–gel synthesis using Pechini complex.

80 °C.[36] The molar ratio of PMN–PFN/AcOH in the gels was kept at 1/5. The Nb-tartarate-ethylene glycol (Pechini) complex for PMN–PFN synthesis was formed by a reaction of $Nb_2O_5{\cdot}xH_2O$ with tartaric acid (TA) and H_2O_2. The obtained solution was dried at 80 °C and dissolved in ethylene glycol (EG) (the molar ratio of EG/TA = 5.5). The acetate solutions were mixed at 80 °C with the Pechini complex to obtain the organic mixture ($(1-x)$PMN–xPFN stoichiometry which represents organic sol) with molar ratio of Pb:Mg:Nb = 1:1/3:2/3 (PMN) and Pb:Fe:Nb = 1:1/2:1/2 (PFN). Viscous PMN–PFN gels were calcined at 600 °C for 2 h in air after 12 h polycondensation (at 25 °C) followed by drying at 100 °C for 8 h. After an uniaxial pressing into tablet form, PMN–PFN precursors were sintered in air in closed crucible at the temperature of 1150 °C for 2, 4 and 6 h, 1200 and 1250 °C for 2 h, respectively. Heating and cooling rate were ±5 °C/min.

The phase composition of PMN–PFN materials was analysed by the X-ray diffraction technique (XRD, a model Philips X Pert Pro) using Cu Kα radiation. The volume fraction of the pv phase in PMN–PFN systems (pv [vol.%]) can be calculated as a ratio of the intensites of XRD diffraction peaks from the reflection of (1 1 0) plane of pv phase (I_{pv}), reflection of (2 2 2) plane of py phase (I_{py}) for $Pb_{1.83}Mg_{0.29}Nb_{1.71}O_{6.39}$ and $Pb_3Nb_4O_{13}$, and reflection of (2 0 1) plane of py phase (I_{py}) for $PbFe_8O_{13}$

Table 1
The properties (colors and efficiency w [wt.%]) of the $(1-x)$PMN–xPFN powders obtained sol–gel synthesis

Sample	x	Composition	Sol at 80 °C	Gel at 25 °C	Dried gel at 100 °C	Powder at 600 °C	w[a] (wt%)
1	0.0	PMN	Brown	Brown	Brown	Yellow	38
2	0.1	0.9PMN–0.1PFN	Red	Brown	Brown	Yellow	38
3	0.2	0.8 PMN–0.2PFN	Green	Green	Yellow	Orange	37
4	0.5	0.5PMN–0.5PFN	Green	Brown	Yellow	Orange	41
5	1.0	PFN	Red	Orange	Green	Red	42

[a] See text.

according to Eq. (1), respectively.[7]

$$\text{pv}\% = \frac{I_{\text{pv}}}{I_{\text{pv}} + I_{\text{py}}} \times 100 \quad (1)$$

The size and shape of powder particles were observed by a transmission electron microscopy (TEM, a model TESLA BS 500). The microstructures of the ceramic samples were characterized using a scanning electron microscope (SEM, a model TESLA BS 340) equipped with an energy dispersive X-ray (EDX) analyser LINK ISIS and by the optical microscopy. The bulk densities of the final sintered ceramics were measured geometrically after polishing. The relative permitivity of the ceramic samples were measured using HP 4194A impedance analyser at room temperature at frequency of 1 kHz after coating of both sides of the samples by Ag paste.

3. Results and discussion

Using the sol–gel synthesis, five different types of $(1-x)$PMN–xPFN systems were prepared by the variation of $x = 0.0, 0.1, 0.2, 0.5$ and 1.0 (see Table 1). Table 1 summarizes the properties colors and efficiency of PMN–PFN powder systems (denoted as 1, 2, 3, 4 and 5), where efficiency $w = (x/y) \times 100$, x is mass of obtained powder after calcination of gel and y is theoretical mass of powder according to initial stoichiometry $(1-x)$PMN–xPFN.

XRD diffractograms of calcined PMN–PFN powders (1, 4 and 5) prepared at 600 °C are shown in Fig. 2. In the sample 1 (Fig. 2a), the pure pyrochlore (py) phase $Pb_{1.38}Nb_{1.71}Mg_{0.29}O_{6.39}$ (JCPDS 37-0071, PMN py phase) was present only. In the sample 4 (Fig. 2b), the mixture of two pyrochlore $Pb_3Nb_4O_{13}$ (JCPDS 25-443) and $Pb_{1.38}Nb_{1.71}Mg_{0.29}O_{6.39}$ phases were present. It is very complicated to distinguish and to confirm that the sample 5 (Fig. 2c) is composed from single py phase (e.g. $Pb_3Nb_4O_{13}$) or more py phases because of larger half width of peaks in the maximum (small particle size) in XRD records. Calcined powders with fine pyrochlore phase were prepared from Nb-ethylene glycol-tartarate complex with the molar ratio of EG/TA = 5.5 and with pure perovskite phase with EG/TA = 12 and molar ratio $TA/Nb^{5+} = 2/1$.[5,14] The content of py phase in the PMN calcined powders prepared by sol–gel process using complex of niobium with molar ratio EG/TA = 10 decreased from single py phase to

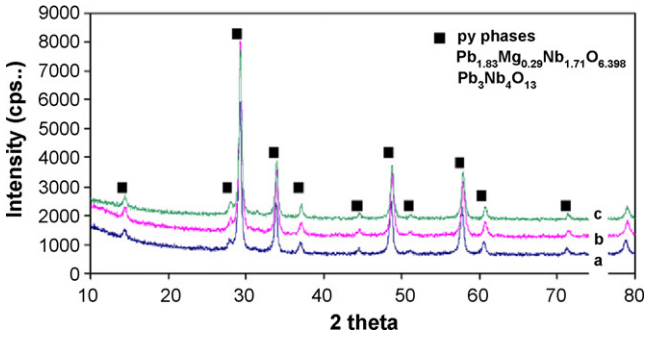

Fig. 2. XRD diffractograms of the $(1-x)$PMN–xPFN powders calcined at 600 °C (a) PMN, (b) 0.5PMN–0.5PFN, and (c) PFN (samples 1, 4 and 5).

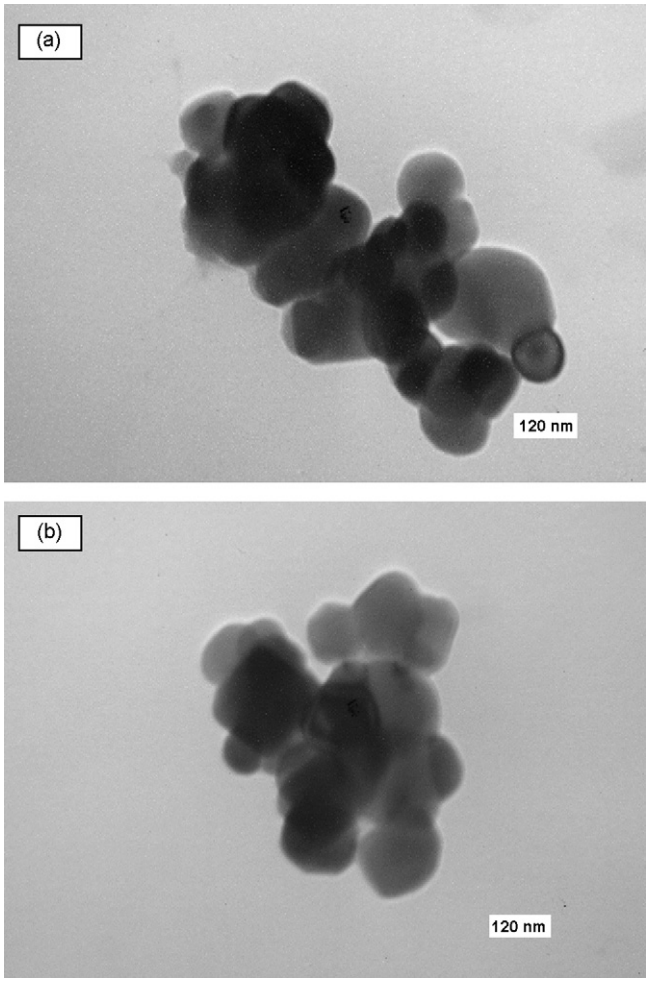

Fig. 3. TEM micrograph of the calcined powder: (a) PMN (sample 1) and (b) PFN (sample 5).

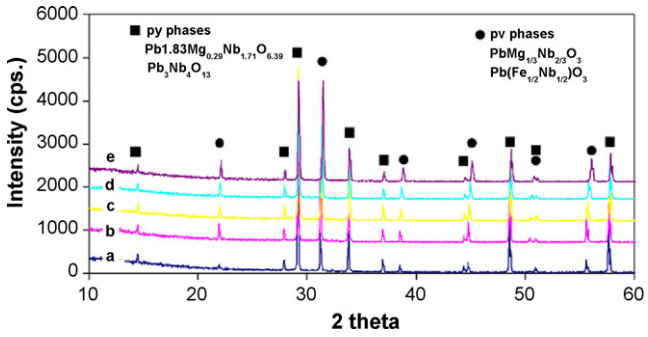

Fig. 4. XRD diffractograms of the $(1-x)$PMN–xPFN ceramics sintered at 1150 °C for 2 h: (a) PMN, (b) 0.9PMN–0.1PFN, (c) 0.8PMN–0.2PFN, (d) 0.5PMN–0.5PFN, and (c) PFN (samples 1–5).

∼40 vol.%.[37] The TEM images of calcined powders (samples 1 and 5) are shown in Fig. 3a and b. The particles have almost spherical shape with the average particle size of 80–120 nm in pure PMN and 100–150 nm in pure PFN powders.

XRD diffractograms of the final PMN–PFN ceramics 1–5 after sintering of powder calcined systems at 1150 °C for 2 h are shown in Fig. 4a–e. In the sample 1 (Fig. 4a), the PMN perovskite (pv) phase $Pb(Mg_{1/3}Nb_{2/3})O_3$ (JCPDS 27-1199) and pyrochlore $Pb_{1.38}Nb_{1.71}Mg_{0.29}O_{6.39}$ phase were present. In the samples 2–5 (Fig. 4b–e), the PFN perovskite phase $Pb(Fe_{1/2}Nb_{1/2})O_3$ (JCPDS 32-522) and pyrochlore $Pb_3Nb_4O_{13}$ phase were found. The highest reflexion of perovskite (pv) phase as a result from the comparison of ceramic samples were observed in the PFN ceramic sample 5. For any sintering time, the mixture of py and pv phases were always found in the sample. XRD diffractograms of the PMN–PFN ceramics 1–5 sintered at 1150 °C for 6 h are shown in Fig. 5a–e. From comparison ceramic samples sintered at the same temperature but for different times results, that the decrease in intensities of peaks from pv phase (rapid in the sample 5) was found in XRD records only. Novel py phases as $PbFe_8O_{21}$ (JCPDS 14-79) or $Pb_2Fe_{1.5}Nb_{0.5}O_{5.5}$ (JCPDS 18-22) are formed in pure PFN ceramics for longer sintering times.

Tables 2 and 3 summarize the volume fractions of pv phase in the ceramic samples, their densities and relative dielectric permitivities, ε_r, at 25 °C (at frequency 1 kHz) as a function of sintering

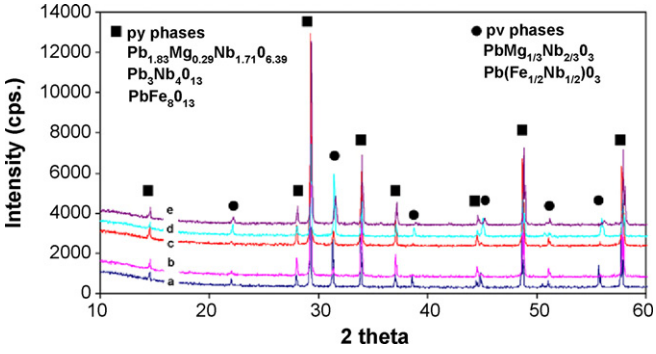

Fig. 5. XRD diffractograms of the $(1-x)$PMN–xPFN ceramics sintered at 1150 °C for 6 h (a) PMN, (b) 0.9PMN–0.1PFN, (c) 0.8PMN–0.2PFN, (d) 0.5PMN–0.5PFN, and (c) PFN (samples 1–5).

Table 2
The volume content of perovskite phase of PMN–PFN ceramics sintered at 1150–1250 °C

Sample	pv phase (vol.%)				
	1150 °C			1200 °C	1250 °C
	2 h	4 h	6 h	2 h	2 h
1	26	39	32	36	31
2	46	–	9	–	–
3	31	–	10	35	–
4	41	44	41	42	–
5	50	51	16	38	–

temperature and time. The content of pv phase in PMN–PFN samples was calculated according to Eq. (1). Significant effects of increasing sintering temperature on phase formation and densification were found. In PMN powder composed from pure py phase (sample 1), the content of pv phase increased up to ∼39 vol.% after sintering at 1150 °C for 4 h. The maximal content of pv phase ∼51 vol.% was found in the ceramic sample 5 sintered at 1150 °C for 4 h. In all samples, the content of pv phase in long time sintering process (6 h) decreased. The maximum bulk density increased (from 4.6 to 6.3 g/cm^3) with increasing both the PFN content and sintering temperature. The optimum sintering temperature for the preparation of PMN–PFN ceramics is shifted from 1200 to 1150 °C as follows from the comparison of values of porosities and pv content in the samples. The maximum density (6.7 g/cm^3) was obtained in 0.5PMN–0.5PFN ceramics at 1150 °C for 6 h. From the Table 3 follows that the relative dielectric permitivity, ε_r, is mainly sensitive to the pyrochlore formation and densification process during sintering. Low value of ε_r was measured in the low density samples with high pyrochlore contents (paraelectric py phase at room temperature, i.e. $\varepsilon_r \sim 130$ for $Pb_{1.38}Nb_{1.71}Mg_{0.29}O_{6.39}$).[35] There are many significant factors such as e.g. sintering time, pyrochlore phase distribution, pore size distribution or the Curie temperature, on which ε_r will depend.

Distribution of pores and pore size in the final ceramic samples sintered at 1150 and 1200 °C (1250 °C in the case of sample 1 (pure PMN)) are visible in Fig. 6. Large irregular pores with the size up to 50 μm can be observed in the microstructure of polished ceramic sample 1 in Fig. 6a. In the microstructure, rectangular and triangular shaped grains are visible with

Table 3
The density ρ (g/cm^3) of polished pelets PMN–PFN ceramics and relative dielectric permitivity (ε_r) measured at 25 °C and frequency 1 kHz

Sample	ρ (g/cm^3)					ε_r (1 kHz)	
	1150 °C			1200 °C	1250 °C	1150 °C	
	2 h	4 h	6 h	2 h	2 h	2 h	6 h
1	4.6	5.3	4.5	5.5	6.4	93	256
2	4.9	5.7	5.5	6.1	–	78	160
3	5.1	6.0	5.8	6.2	–	96	169
4	5.1	6.2	6.7	6.3	–	275	34443
5	–	6.0	5.7	6.1	–	–	16784

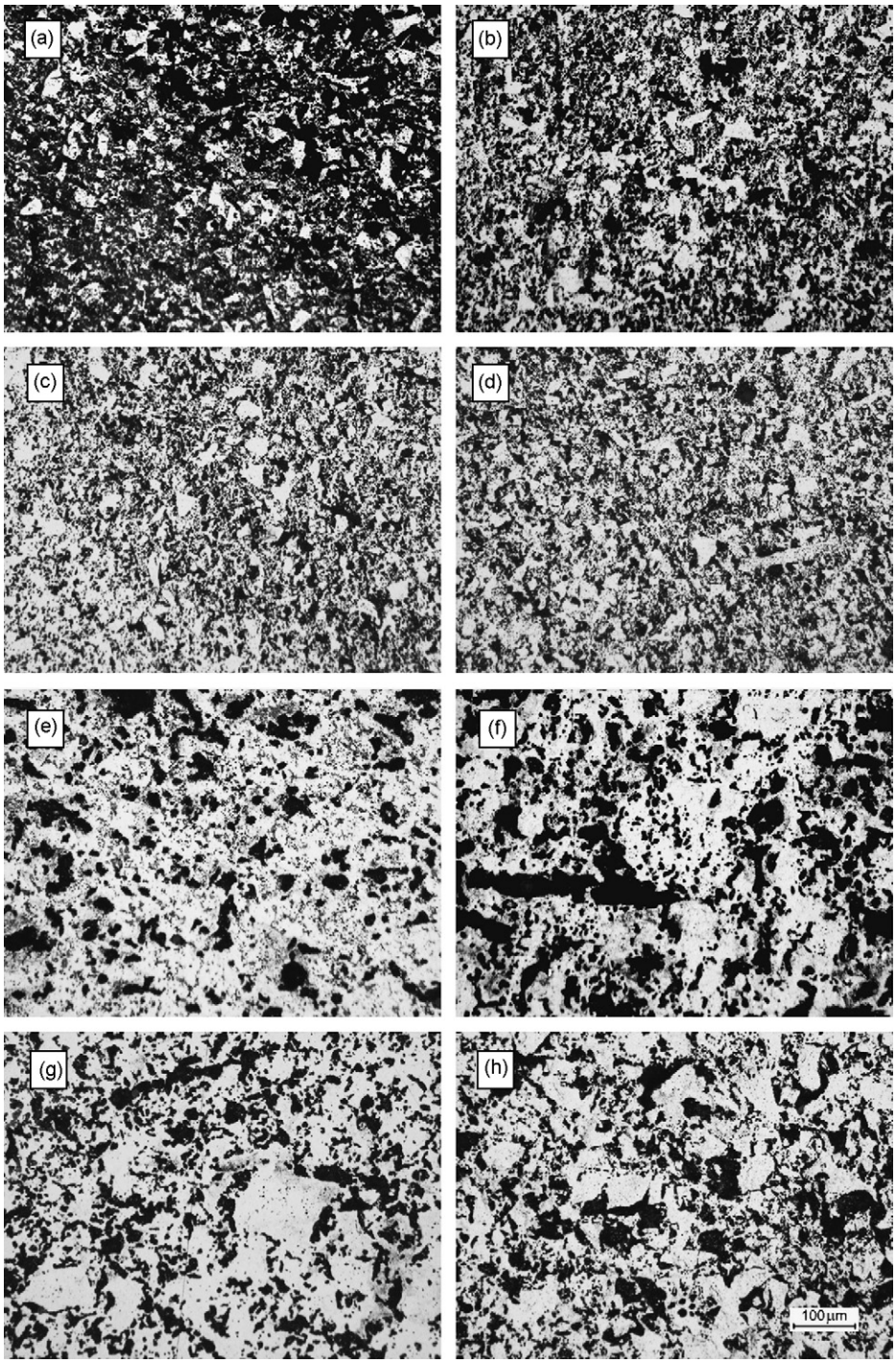

Fig. 6. Optical micrographs of the polished surfaces of ceramic samples sintered at 1150 °C/4 h ((a) sample 1, (b) sample 5, (c) sample 4, (d) sample 2) and 1200 °C/2 h ((f) sample 5, (g) sample 4, (h) sample 2), 1250 °C/2 h ((e) sample 1).

average grain size up to 80 μm, which correspond with various sections of randomly oriented grains of the pyrochlore or perovskite phases of the cubic symmetry. Similar types of grains were observed in all microstructures of the ceramic samples sintered at the same conditions (1150 °C/4 h) (Fig. 6a–d). Area pore distribution was the largest in the sample 1 (∼42%) and the lowest (21%) in the sample 4 whereas only a very low portion of larger pores were found in the microstructures of samples which contain of PFN phase. The observed pore distributions and area porosities are in accordance with measured values of densities (see Table 3). The significant change in the pore shape was found after sintering of the sample 1 at 1250 °C, where pores obtained more spherical character. The pore size was from 10 to 70 μm whereas the rectangular grains can be distinguished in the microstructure. The high fraction of larger (70 μm) so as small (10–20 μm) pores on

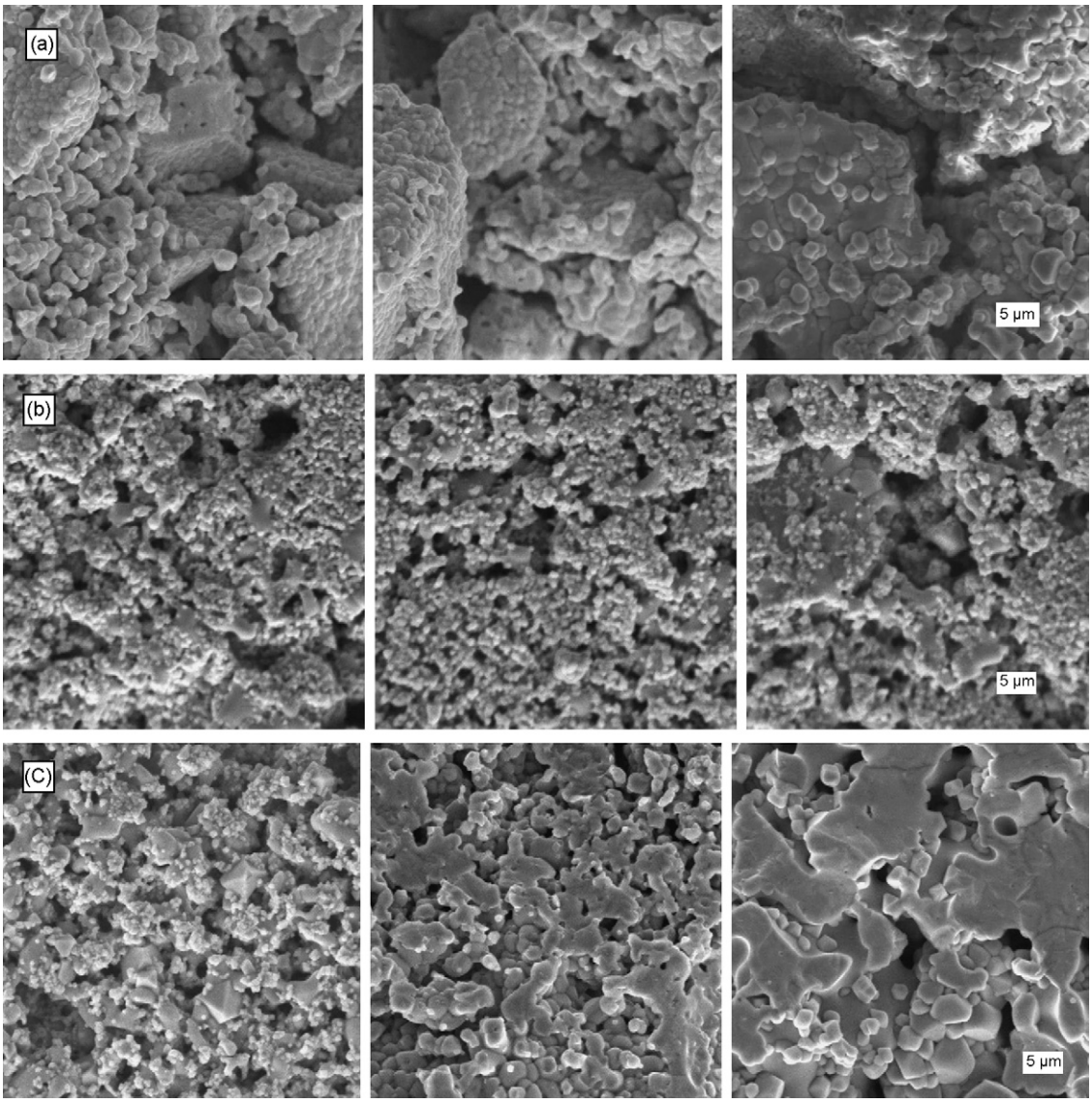

Fig. 7. SEM micrographs of fracture surfaces of the PMN–PFN ceramics sintered at the temperature of 1150 °C with different time for 2, 4 and 6 h (a) PMN, (b) 0.5PMN–0.5PFN, and (c) PFN.

the total porosity was observed in samples sintered at 1200 °C which contain PFN phase, while the total area fraction of pores was between 20 and 30%. In pure PFN ceramics, the pores are rectangular distributed in the microstructure. In samples PMN–PFN, the regular shaped grains are clearly visible in microstructures—thus, pores are eliminated from the interior of grains into grain boundaries with simultaneous grain growth up to >100 μm (Fig. 6g).

Microstructures of fractured PMN–PFN ceramics sintered at the temperature of 1150 °C for 2, 4 and 6 h are shown in Fig. 7. The microstructure of ceramic sample 1 (pure PMN) (Fig. 7a) is characterized by almost spherical shaped types of grains with average grain size ∼2 μm after sintering for 2 h. No clear evidence for the presence of octahedral shaped grains of pyrochlore phase was found. The average grain size increases from 2 to 4 μm with increase in the sintering time from 2 to 6 h. Bimodal grain size distribution in 0.5PMN–0.5PFN ceramics (sample 4) can be visible in Fig. 7b. Fine grains are characterized by the globular shape with average grain size of 1 μm. Large grains (3–5 μm) have octahedral shape which is typical for grains of pyrochlore phase ($Pb_{1.38}Nb_{1.71}Mg_{0.29}O_{6.39}$ or $Pb_3Nb_4O_{13}$). The significant change in grain size with sintering time at given temperature was not observed in this sample. In Fig. 7c, the octahedral particles of PMN py phase (∼5 μm size) were observed in the microstructure of sample 5 after sintering for 2 h. Besides, regular or spherical shaped small grains (∼1 μm size) were present in the microstructure at the same sintering conditions. Grain size increases with sintering time in the sample 5 and octahedral shaped grains are not so clear visible in the microstructure. No small grains can be found in microstructure ceramics sintered at 1150 °C for sintering times above 6 h.

The SEM micrographs of polished and etched surface of 0.5PMN–0.5PFN ceramics (sample 4) sintered at 1150 °C for

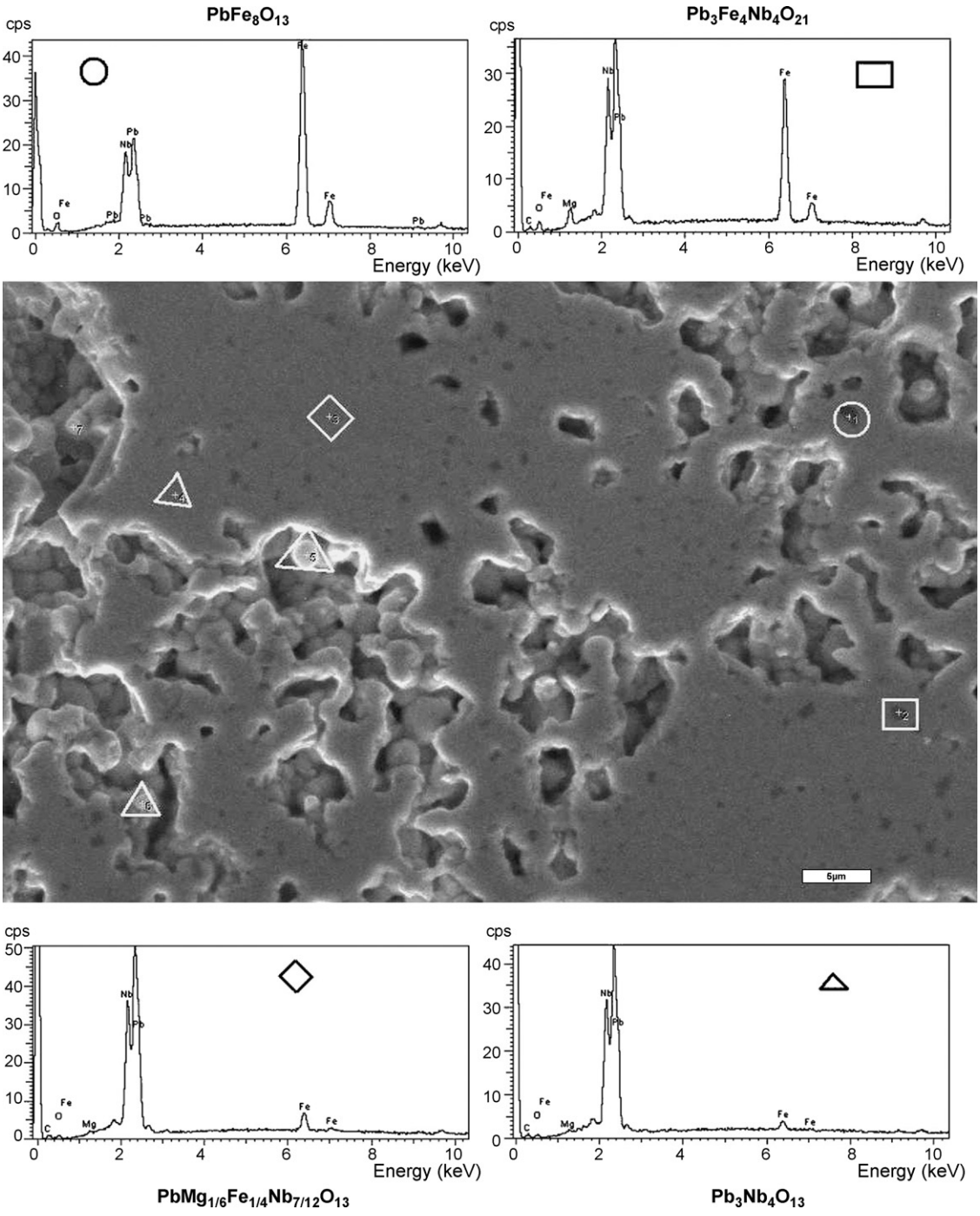

Fig. 8. SEM micrographs of polished and etched surface of 0.5PMN–0.5PFN ceramics sintered at 1150 °C for 4 h with EDX analysis different places with pyrochlore phases: $PbFe_8O_{13}$ (◯), $Pb_3Fe_4Nb_4O_{21}$ (□), $Pb_3Nb_4O_{13}$ (△) and perovskite phase: $Pb(Mg_{1/6}Fe_{1/6}Nb_{7/12}\}O_{13}$ (◊).

4 h with EDX analysis in the some regions are shown in Fig. 8. The results of analysis showed that the more complex types of py phases are present in ceramics which are very hardly distinguished in XRD spectra. The effect of sintering temperature on grain growth in sample 1 is demonstrated in Fig. 9a and b. Average grain size in the ceramics rose from 3 to 7 μm with increasing in sintering temperature from 1200 to 1250 °C. High volume fraction of grains of py PMN phase is visible in Fig. 8 which is in accordance with results of XRD analysis.

Sintering temperature of 1150 °C and sintering time of 4 h represent optimal conditions for the tranformation pyrochlore phases in PMN–PFN powders to the perovskite phase. Maximal densities in final ceramics were found for sintering time of 4 h and maximal value of ε_r were measured in these samples after sintering for 6 h.

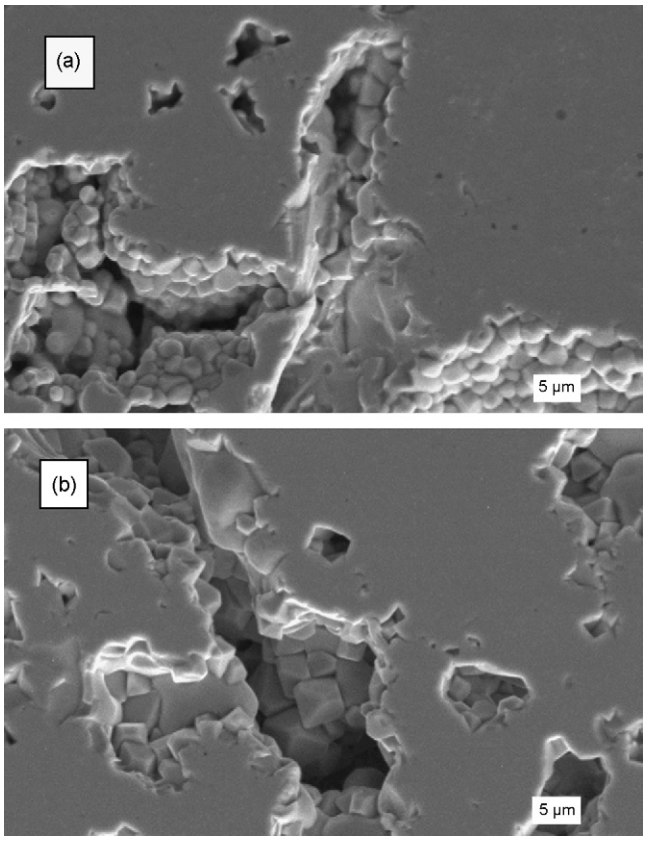

Fig. 9. SEM micrographs of etched polished surfaces of PMN ceramics sintered at (a) 1200 °C for 2 h and (b) 1250 °C for 2 h.

4. Conclusion

$(1-x)$PMN–xPFN ceramics, where $x = 0.0$–1.0, were prepared using sol–gel synthesis by mixing acetates Pb, Mg and Fe with Nb-ethylene glycol-tartarate complex, calcination of gels at 600 °C and sintering at temperatures from 1150 to 1250 °C for various times. The pure pyrochlore phases ($Pb_{1.83}Mg_{0.29}Nb_{1.71}O_{6.39}$ or $Pb_3Nb_4O_{13}$) was created by the calcination at 600 °C. Average size of particles of pure PMN and PFN calcinated powders was ~80 and ~150 nm. The maximum bulk density in ceramic samples increased with both sintering temperature and the content of PFN phase in samples but the volume fractions of porosity were too high in the prepared samples. From the point of view of perovskite phase content, the optimum sintering temperature of PMN–PFN is shifted from 1200 to 1150 °C.

In the microstructures of PMN–PFN ceramics sintered at 1150 °C at different time, the bimodal grain size distribution was found with small grains of globular shape and larger grains of regular or octahedral shape. The results of EDX and XRD analysis showed that the more complex types of pyrochlore phases were present in ceramics.

Acknowledgement

This work was supported by the Grant Agency of the Slovak Academy of Sciences through project No. 2/5145/25.

References

1. Uchino, K., Nomura, S., Cross, L. E., Jang, S. J. and Newnham, R. E., Electrostrictive effect in lead magnesium niobate single crystals. *J. Appl. Phys.*, 1980, **51**, 1142–1145.
2. Jang, S. J., Uchino, K., Nomura, S. and Cross, L. E., Electrostrictive behavior of lead magnesium niobate based ceramic dielectrics. *Ferroelectrics*, 1980, **27**, 31–34.
3. Uchino, K., Electrostrictive actuators: materials and applications. *Am. Ceram. Soc. Bull.*, 1986, **65**, 647–652.
4. Swartz, S. L., Shrout, T. R., Schulze, W. A. and Cross, L. E., Dielectric properties of lead magnesium niobate ceramics. *J. Am. Ceram. Soc.*, 1984, **67**, 311–315.
5. Smolenskii, G. A. and Agranovskaya, A. I., Dielectric polarization and losses of some complex compounds. *Sov. Phys. Tech. Phys.*, 1958, **3**, 1380–1382.
6. Lejeune, M. and Boilot, J. P., Formation mechanism and ceramic process of the ferroelectric perovskites: $Pb(Mg_{1/3}Nb_{2/3})O_3$ and $Pb(Fe_{1/2}Nb_{1/2})O_3$. *Ceram. Int.*, 1982, **8**, 99–103.
7. Swartz, S. L. and Shrout, T. R., Fabrication of perovskite lead magnesium niobate. *Mater. Res. Bull.*, 1982, **17**, 1245–1250.
8. Guha, J. P. and Anderson, H. U., Preparation of perovskite $Pb(Mg_{1/3}Nb_{2/3})O_3$ using $Pb_3Nb_2O_8$ and MgO. *J. Am. Ceram. Soc.*, 1986, **69**, C-287–C-288.
9. Chaput, F., Boilot, J. P., Lejeune, M., Papiernik, R. and Pfalzgraf, L. G. H., Low-temperature route to lead magnesium niobate. *J. Am. Ceram. Soc.*, 1989, **72**, 1355–1357.
10. Katayama, K., Abe, M. and Akiba, T., Preparation of $Pb(Mg_{1/3}Nb_{2/3})O_3$ powder by molten salt method. *Ceram. Int.*, 1989, **15**, 289–295.
11. Ananta, S. and Thomas, N. W., A modified two-stage mixed oxide synthetic route to lead magnesium niobate and lead iron niobate. *J. Eur. Ceram. Soc.*, 1999, **19**, 155–163.
12. Jun, S. G., Kim, N. K., Kim, J. J. and Cho, S. H., Synthesis of perovskite ceramics PMN–PFN via B-site precursors and their dieletric properties. *Mater. Lett.*, 1998, **34**, 336–340.
13. Ravindranathan, P., Komarneni, S. and Roy, R., Solid-state epitaxial effects in structurally diphasixc xerogel of $Pb(Mg_{1/3}Nb_{2/3})O_3$. *J. Am. Ceram. Soc.*, 1990, **73**, 1024–1025.
14. Jenhi, M., Ghadraoui, E. H. E., Balli, H., Aatmani, M. E. and Rafiq, M., Synthesis and characterization of $Pb(Fe_{0.5}Nb_{0.5})O_3$ by sol–gel and solid-state method. *Ann. Chim. Sci. Mater.*, 1998, **23**, 151–154.
15. Francis, L. F., Oh, Y. and Payne, D. A., Sol–gel processing and properties of lead magnesium niobate powders and thin layers. *J. Mater. Sci.*, 1990, **25**, 5007–5013.
16. Yoon, K. H., Park, J. H. and Kang, D. H., Characteristics of lead magnesium niobate thin film prepared by sol–gel processing using a complexing agent. *J. Am. Ceram. Soc.*, 1995, **78**, 2267–2270.
17. Yoshikawa, Y. and Uchino, K., Chemical preparation of lead-containing niobate powders. *J. Am. Ceram. Soc.*, 1996, **79**, 2417–2421.
18. Narendar, Y. and Messing, G. L., Kinetic analysis of combustion synthesis of lead magnesium niobate from metal carboxylate gels. *J. Am. Ceram. Soc.*, 1997, **80**, 915–924.
19. Sekar, M. M. A., Halliyal, A. and Patil, K. C., Synthesis, characterization, and properties of lead-based relaxor ferroelectrics. *J. Mater. Res.*, 1996, **11**, 1210–1218.
20. Yoon, K. H., Cho, Y. S., Lee, D. H. and Kang, D. H., Powder characteristic of $Pb(Mg_{1/3}Nb_{2/3})O_3$ prepared by molten salt synthesis. *J. Am. Ceram. Soc.*, 1993, **76**, 1373–1376.
21. Choy, J. H., Yoo, J. S., Kang, S. G., Hong, S. T. and Kim, D. J., Ultrafine $Pb(Mg_{1/3}Nb_{2/3})O_3$ (PMN) powder synthesised from metal citrate gel by thermal shock method. *Mater. Res. Bull.*, 1990, **25**, 283–291.
22. Carvalho, J. C., Paiva-Santos, C. O., Zaghete, M. A., Oliveria, C. F., Varela, J. A. and Longo, E. J., Phase analysis of seeded and doped $Pb(Mg_{1/3}Nb_{2/3})O_3$ prepared by organic solution of citrates. *Mater. Res.*, 1996, **11**, 1795–1799.
23. Gupta, S. M. and Kulkarni, A. R., Synthesis of perovskite lead magnesium niobate using partial oxalate method. *Mater. Res. Bull.*, 1993, **28**, 1295–1301.

24. Camargo, E. R., Kakihana, M., Longo, E. and Leite, E. R., Pyrochlore-free $Pb(Mg_{1/3}Nb_{2/3})O_3$ prepared by a combination of the partial oxalate and the polymerized complex methods. *J. Alloys Compd.*, 2001, **314**, 140–146.
25. Cavalheiro, A. A., Zaghete, M. A., Paiva-Santos, C. O., Varela, J. A. and Longo, E., Influence of synthesis and processing parameters of the columbite precursor on the amount of perovskite PMN. *Mater. Res.*, 1999, **2**, 255–260.
26. Das, R. N. and Pramamik, P., Single step chemical synthesis of lead based relaxor ferroelectric niobate fine powders. *NanoStruct. Mater.*, 1999, **11**, 325–330.
27. Das, R. N. and Pramamik, P., Chemical synthesis of fine powder of lead magnesium niobate using niobium tartarate complex. *Mater. Lett.*, 2000, **46**, 7–14.
28. Cavalheiro, A. A., Foschini, C. R., Zaghete, M. A., Paiva-Santos, C. O., Cilense, M., Varela, J. A. and Longo, E., Seeding of PMN powders made by the Pechini method. *Ceram. Int.*, 2001, **27**, 509–515.
29. Larbot, A., Bali, H., Rafiq, M., Julbe, A., Guizard, C. and Cot, L., Elaboration and characterization of lead perovskites from colloidal solution. *J. Non-Cryst. Solids*, 1992, **147–148**, 74–79.
30. Costa, A. L., Galassi, C., Fabbri, G., Roncari, E. and Capiani, C., Pyrochlore phase and microstructure development in lead magnesium niobate materials. *J. Eur. Ceram. Soc.*, 2001, **21**, 1165–1170.
31. Mergen, A. and Lee, W. E., Fabrication, characterization and formation mechanism of $Pb_{1.83}Mg_{0.29}Nb_{1.71}O_{6.39}$ pyrochlore. *J. Eur. Ceram. Soc.*, 1997, **17**, 1033–1047.
32. Ananta, S. and Thomas, N. W., Relationships between sintering conditions, microstructure and dielectric properties of lead magnesium niobate. *J. Eur. Ceram. Soc.*, 1999, **19**, 629–635.
33. Gupta, S. M. and Kulkarni, A. R., Dielectric and microstructure studies of lead magnesium niobate prepared by partial oxalate route. *J. Eur. Ceram. Soc.*, 1996, **16**, 473–480.
34. Ananta, S. and Thomas, N. W., Relationships between sintering conditions, microstructure and dielectric properties of lead iron niobate. *J. Eur. Ceram. Soc.*, 1999, **19**, 1873–1881.
35. Ananta, S. and Thomas, N. W., Fabrication of PMN and PFN ceramics by a two-stage sintering technique. *J. Eur. Ceram. Soc.*, 1999, **19**, 2917–2930.
36. Brunckova, H., Medvecky, L., Briancin, J. and Saksl, K., Influence of hydrolysis conditions of the acetate sol–gel process on the stoichiometry of PZT powders. *Ceram. Int.*, 2004, **30**, 453–460.
37. Briancin, J., Brunckova, H. and Medvecky, L., Acetate sol–gel synthesis of PMN ceramics from Nb-ethyleneglycol-tartarate complex. *Ferroelectrics*, 2005, **319**, 11–17.